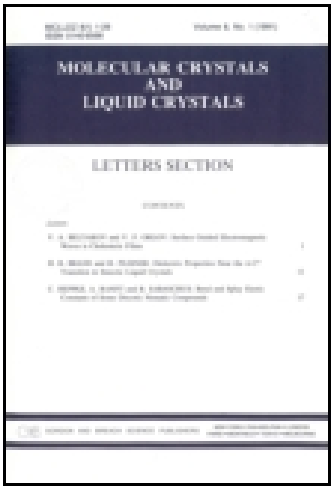

Molecular Crystals and Liquid Crystals
Publication details, including instructions for authors and subscription information:
http://www.tandfonline.com/loi/gmcl20

Phenomenological Interpretation of Impedance/Capacitance Measurements on Organic Electronic Devices Under Illumination

L. F. Santos [a] & C. J. Pereira [a]
[a] Departamento de Física , Universidade Estadual Paulista - UNESP , São José do Rio Preto , SP , 15054-000 , Brazil
Published online: 28 Mar 2014.

To cite this article: L. F. Santos & C. J. Pereira (2014) Phenomenological Interpretation of Impedance/Capacitance Measurements on Organic Electronic Devices Under Illumination, Molecular Crystals and Liquid Crystals, 589:1, 74-82, DOI: 10.1080/15421406.2013.872344

To link to this article: http://dx.doi.org/10.1080/15421406.2013.872344

Mol. Cryst. Liq. Cryst., Vol. 589: pp. 74–82, 2014

ISSN: 1542-1406 print/1563-5287 online
DOI: 10.1080/15421406.2013.872344

Taylor & Francis
Taylor & Francis Group

Phenomenological Interpretation of Impedance/Capacitance Measurements on Organic Electronic Devices Under Illumination

L. F. SANTOS* AND C. J. PEREIRA

Departamento de Física,Universidade Estadual Paulista – UNESP, São José do Rio Preto, SP 15054-000, Brazil

The electrical properties of organic electronic devices based on poly(2-methoxy-5-(3',7'-dimethyloctyloxy)-1,-phenylene vinylene) as the active layer were studied under light-excitation at different wavelength ranges and intensities, with particular focus on the frequency-response of the complex capacitance. To interpret the obtained results, an adaptation of abrupt cut-off frequency analysis of the capacitance data was developed considering the displacement of the quasi-Fermi levels due to the incidence of light. The application of such formalism allowed the determination of the position of the bulk Fermi level, the Debye length associated to the photo-generated charge-carriers and the displacement on the quasi-Fermi levels due to illumination.

Keywords Impedance/capacitance spectroscopy; organic electronic devices; photoconductivity; conjugated polymers; OLEDs

Introduction

Organic/polymeric electronic/optoelectronic devices have been studied and improved continuously in the latest two decades, achieving, at the moment, a high level of sophistication, resolution, performance and efficiency. They present several advantages compared to devices based on inorganic semiconductors, as light-weight, flexibility, ease of processing, capacity of covering large areas and the possibility to tune the bandgap energy in almost the entire visible spectrum. However, in spite of the advantages, there are still some drawbacks that limit the application of organic devices in large scale, mainly related to stability or to lifetime. One of these problems is associated to the formation of trap states during the photo-generation process. These states can strongly influence the charge-carrier mobility as well the charge recombination efficiency in the organic semiconductor active layer, being deleterious to the performance of all sort of organic electronic devices: light-emitting diodes (OLEDs), solar cells (OPVs) and field-effect transistors (OFETs).

The influence of light on the electrical behavior of organic semiconductors has been largely studied [1-6] by considering the spectral d.c. response of the photocurrent of organic devices in OLED structures. Other authors have, however, focused the dynamics of the charging/decharging processes in organic semiconductors, which are better described by using impedance/capacitance spectroscopy technique [7–9]. The behavior of the

*Address correspondence to L. F. Santos. Phone: +55 17 3221-2388; Fax: +55 17 3221-2247; Email: lucas@sjrp.unesp.br

capacitance spectrum on frequency is particularly interesting to analyze the properties of localized states that dwell in the semiconductor bandgap.

Abrupt cut-off models, which consider that only states localized further a certain position associated to a critical angular frequency, are able to respond promptly to an electric field a.c. modulation, have been successfully applied to the interpretation of the dispersion in frequency of the capacitance spectra obtained from devices comprising a rectifying junction formed between a semiconductor and a metal [10-13]. This method has been used to investigate the charging dynamics processes in inorganic semiconductors [10-11], organic molecular solids [12] and polymers [13].

In the present work, an adaptation of the abrupt cut-off frequency analysis is made in order to incorporate the results of capacitance spectra from polymeric diodes under illumination, by considering the effect of the displacement of the quasi-Fermi levels of the organic semiconductor due to incidence of light.

Theory

In a rectifying junction - like the one formed between an organic semiconductor and a metal which work function is far away from either the HOMO or the LUMO levels - when a small a.c. modulation and no d.c. bias is applied (i.e. close to the equilibrium), the states which can have their occupancy changed during the impedance/capacitance measurement are those which cross the Fermi level (E_F) at a certain distance x from the junction. In this picture, considering a continuum of gap states, the states which follow the a.c. modulation will be comprised between E_F and a maximum energy level E_m, which is parallel to the corresponding band edge (HOMO or LUMO) and crosses the Fermi level at the semiconductor/metal interface [11, 13]. Moreover, these states don't have the same response time, since each one crosses the Fermi level at a position x. The response time of these states is due to the exchange of charge carriers with the corresponding band. Considering a p-type organic semiconductor, this time is given by:

$$\frac{1}{\tau_F(x)} = 2\nu_p \exp\left(-\frac{(E_F - E_B)(x)}{k_B T}\right) \tag{1}$$

where ν_p is the attempt-to-escape frequency for the holes trapped at E_F, E_B is the LUMO level and k_B is the Boltzmann constant.

Considering that x_ω is the position given by Eq. 1 for the $\omega\tau = 1$ condition (Debye relaxation), the states which cross E_F before x_ω cannot respond to the a.c. modulation, whereas those which cross E_F after x_ω are immediately probed by the alternating field. The equivalent capacitance of the device can be considered as being composed by two contributions, in a series association: one given by $k\varepsilon_0 A/x_\omega$, for which the device responds as an ideal dielectric and a second one given by $k\varepsilon_0 A/L_\omega$, where A is the device area, $k\varepsilon_0$ is the electrical permittivity of the semiconductor and L_ω is a characteristic length associated to the states that can follow the a.c. modulation at the frequency ω. The abrupt cut-off frequency model assumes that only frequencies in the vicinity of or below an angular frequency $\omega_0 = 1/\tau_F$(bulk) contribute to L_ω. As consequence, only the states below the bulk Fermi level position will follow the a.c. modulation. In this picture, $L_\omega = L_D$, where L_D is the Debye length associated to the states at the bulk Fermi level. The total capacitance can then be given by [11]:

$$C = \frac{k\varepsilon_0 A}{(x_\omega + L_D)} \tag{2}$$

From the exposed above and considering that, for a constant DOS around the Fermi level, the spatial dependence of the electrostatic potential can be considered to have an exponential dependence, with characteristic length L_D, Eq. 1 and 2 can be combined to derive the following relationship:

$$\left[\frac{d(k\varepsilon_0 A/C)}{d(\ln\omega)}\right]^{-1} = \frac{1}{L_D}(\ln\omega_0 - \ln\omega) \tag{3}$$

This form is particularly interesting because the left side of the equation can be obtained directly from the experimental results from the capacitance spectra and it presents a linear dependence on *ln* ω. From the data, it is possible to obtain directly the value of L_D (from the angular coefficient of the plot) and of ω_0, from the linear coefficient.

However, if the bulk Fermi level position is too deep in the bandgap, or the space-charge density associated to the Schottky junction is too low, the cut-off frequency is situated in the very low frequency range and the capacitance spectrum of the device is similar to a dielectric material and practically no dispersion in frequency is observed. Conversely, if the device is illuminated by light with wavelength associated to energies higher than the bandgap, charge carriers can be photogenerated in the bulk, shifting the quasi-Fermi levels. The displacement in the quasi-Fermi level position is given by:

$$n^* = n_0 \exp\left(\frac{E_F^* - E_F}{k_B T}\right) \tag{4}$$

where n^* is the photogenerated free charge-carrier density, n_0, the intrinsic charge-carrier density and $E_F{}^*$, the position of the quasi-Fermi level due to illumination.

In this new condition, it is plausible to consider that the response time to the a.c. modulation will be given by the exchange between the correspondent band and the shifted quasi-Fermi level. Combining Eq. 1 and Eq. 4, one can obtain

$$\omega_0 = 2\nu_p \frac{n^*}{n_0} \exp\left(-\frac{(E_F - E_B)(x)}{k_B T}\right) \tag{5}$$

for the cut-off frequency. Eq. 5 shows that, with incidence of light, the ratio n^*/n_0, which is always higher than the unity, can bring the cut-off frequency to higher values of frequency, becoming possible to be observed experimentally.

Experimental Details and Methods

The studied electronic devices were built in a conventional sandwich-like organic light-emitting diode structure (OLED). The device active layers were composed by poly(2-methoxy-5-(3',7'-dimethyloctyloxy)-1,-phenylene vinylene), MDMO-PPV, films, deposited by spin-coating a 1% (w:w) toluene solution on top of patterned ITO/glass substrates which were previously covered by a spin-coated 50-60 nm thick PEDOT film. After drying the films at 150°C, Mg (100 nm)/Al(100 nm) electrodes were evaporated through appropriate shadow mask under high-vacuum conditions. The crossed area between the metallic and ITO electrodes defined the device area, namely about 10mm^2. The thickness of the MDMO-PPV films ranged between 100 nm and 120 nm, determined by profilometry.

Light-excitation of the devices was carried out by using commercial high-brightness LEDs in four different wavelength ranges. The average wavelengths were 409 nm, 475 nm, 523 nm and 589 nm, all in the range that the conjugated polymer absorbs. Half-intensity

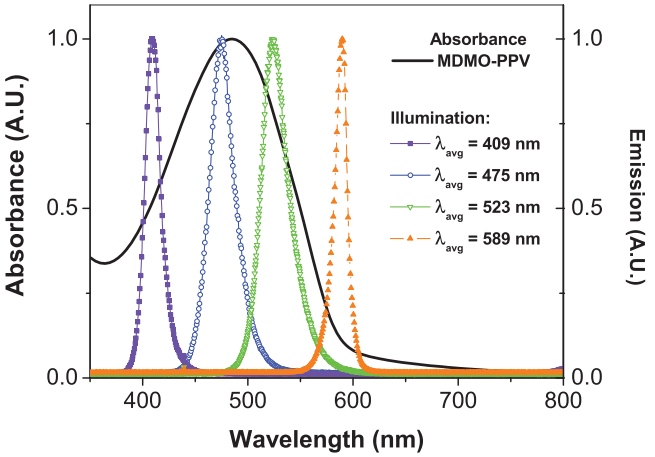

Figure 1. Absorbance spectrum of MDMO-PPV in film and emission spectra of the light sources used to excite the organic device.

bandwidth of the LED spectra ranged between 30 nm and 45 nm. The intensity of the light-excitation was controlled by means the current control of the LEDs and varied in the range between 6 μW/cm^2 and 480 μW/cm^2.

Current-voltage measurements were carried out using a Keithley 6517B electrometer and its coupled voltage source as measure/source unit. Complex impedance/capacitance measurements were carried out by using a Agilent HP 66120A function synthesizer to generate the a.c. modulation and to sweep the frequency in the 1Hz-10^{6}Hz range. The amplitude/phase acquisition was done by computing the signal from either a Stanford SR830 (in the 1Hz-100kHz range) or a lock-in amplifier SR844 (in the 100kHz-1MHz range) after passing through a broadband current-to-voltage amplifier (FEMTO DHPCA-100). Appropriate control through an acquisition software enabled the calculation of any complex dielectric frequency-response function. All the measurements were performed in inert atmosphere (vacuum), inside a metallic chamber with optical windows for light-excitation.

Results and Discussion

Experimental results

Figure 1 shows the absorbance spectrum of a MDMO-PPV film and the emission spectra of the light-sources used to excite the OLEDs. The light-sources with average wavelength at 409 nm, 475 nm and 523 nm present a high overlap with the absorbance spectrum of the OLED active layer, which means high probability of free charge-carrier photo-generation. At $\lambda_{avg} = 589$ nm, the excitation source spectrum intercepts the absorbance spectrum at its low-energy tail, close to the optical bandgap edge, which is about 2.23eV. This indicates that, in the long wavelength range, less photo-generated free charge-carriers will be created and the displacement in the quasi-Fermi levels will much be smaller.

The current-voltage characteristics of a ITO/PEDOT/MDMO-PPV/Mg/Al, in the dark and under different wavelength and intensity excitations, are depicted in Figs. 2a-d. All the curves show typical diode-like characteristics, with a rectification factor of about 1100

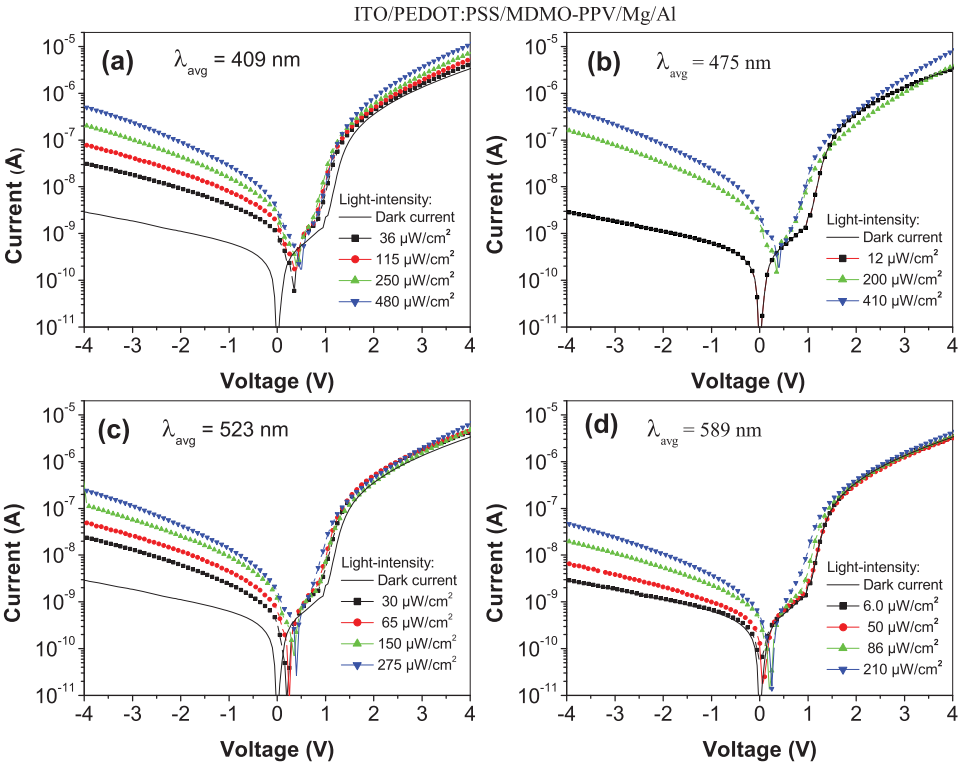

Figure 2. Current-voltage characteristics of the organic device in a ITO/PEDOT/MDMO-PPV/Mg/Al structures at different illumination wavelengths and intensities.

at 4V in the dark. For illumination in practically all wavelength ranges, there is an increase in the current, which is more remarkable when the device is reversely-biased. For excitation in shorter wavelength ranges, especially at 409 nm and 475 nm, more prominent values of short-circuit current and open-circuit voltage are observed, indicating higher free charge-carrier generation and, consequently, a higher displacement in the quasi-Fermi levels position.

The frequency dependence of the real component of the complex capacitance (which is equal to the equivalent capacitance in a parallel RC equivalent circuit), under light-excitation at different wavelength ranges and intensities is shown in Figs. 3a-d. One important feature of these results is that the capacitance spectrum in the dark presents nearly no dispersion in frequency, behaving almost as an ideal dielectric, with a dielectric constant of 3.5. With incidence of light, a much higher number of states are able to cross the quasi-Fermi level in the bulk and follow the a.c. modulation. As consequence, the capacitance of the device becomes frequency-dependent, with a characteristic cut-off frequency given by Eq. 5.

The capacitance spectrum for short-wavelength excitation ($\lambda_{avg} = 409$nm and 475nm) present quite similar behavior. The real capacitance, in the high frequency regime (above 10kHz) is nearly the same as in the dark, since the states which can follow the a.c. modulation are associated to a x_ω abscissa very close to the junction, which means that practically the whole device volume responds as a dielectric. As the frequency decreases, more states in the volume of the semiconductor follow the modulating electric field and

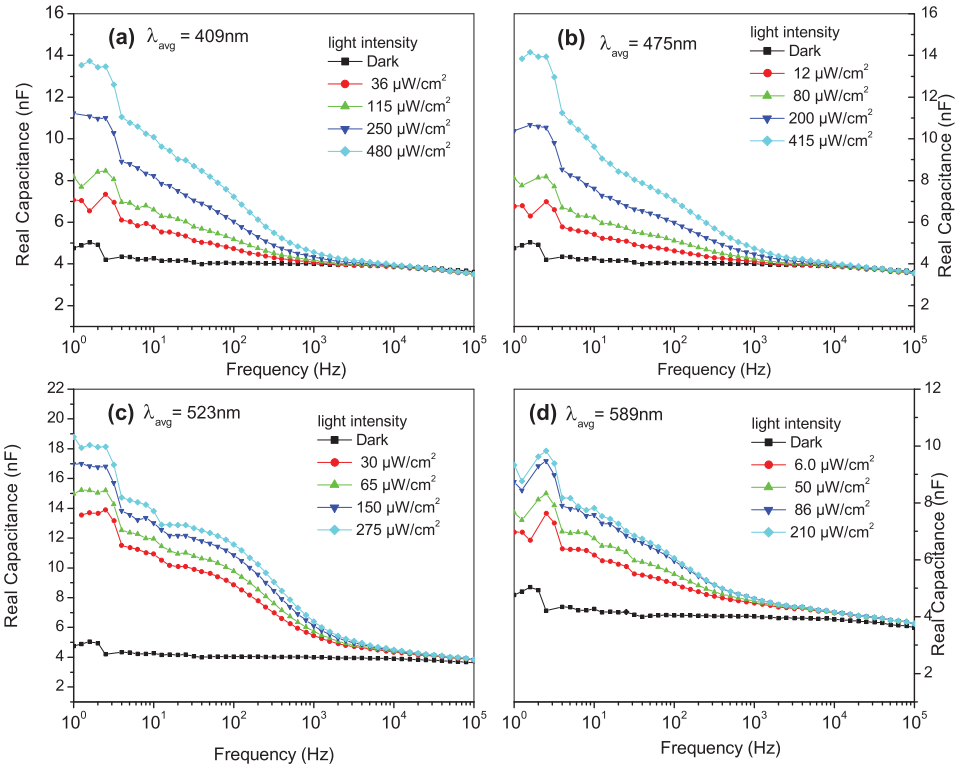

Figure 3. Capacitance spectra obtained from a ITO/PEDOT/MDMO-PPV/Mg/Al device at different illumination wavelengths and intensities.

the capacitance increases, reaching values up to more than 3 times of the high-frequency dielectric capacitance.

Under illumination in the long wavelength range ($\lambda_{avg} = 589$ nm (Fig. 3-d), the device presents lower dispersion in frequency, probably due to the lower free charge-carrier photo-generation, with the maximum capacitance in the low-frequency region achieving about two times the dielectric capacitance in high frequency. For $\lambda_{avg} = 523$ nm (Fig. 3-c), the frequency behavior of the capacitance spectrum presents a slightly higher dispersion and difference in shape compared to the spectra obtained by illumination at shorter wavelengths. The maximum capacitance value, at low frequency, is more than 4 times higher than the dielectric capacitance value. A hypothesis for such different behavior will be discussed in the light of the results obtained from the abrupt cut-off frequency analysis.

Interpretation using abrupt cut-off frequency method

To apply the abrupt cut-off frequency model to the analysis of the experimental results of complex capacitance spectra, it is necessary to assume in the validity of Eqs. 3 and 5, the latest one considering that the device is under illumination. As stated before, the left side of Eq. 3 is supposed to have, in a certain frequency range, a linear dependence with *ln* ω. Application of Eq.3 to the capacitance spectra of the device under illumination of light with

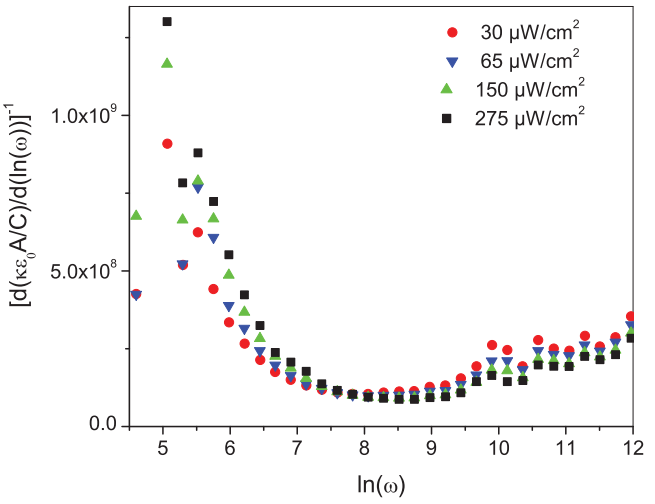

Figure 4. Analysis of the capacitance behaviour using Eq. 3, for different light intensities and for $\lambda_{avg} = 523$ nm.

an average wavelength of 523 nm is presented on Fig. 4. It can be observed that, in the lower angular frequency region, the data follows the expected behavior.

By using Eq. 5 and determining the value of the cut-off frequency from the analysis of the experimental results using Eq. 3, it is possible the determine the value of the ratio of free charge carriers photogeneration (which gives the shift in the quasi-Fermi level by illumination, according to Eq. 4), the Debye length associated to states at the bulk quasi-Fermi level and the bulk Fermi level position.

The results obtained are presented on Table I, for the highest illumination levels, which provided better analysis results. In these calculations, an attempt-to-scape frequency for holes (ν_p) of 1×10^5 rad/s and a bulk Fermi level position, related to the LUMO, of 350meV were used. The ratio between the free photogenerated charge-carriers density and the intrinsic charge-carrier density was estimated from the increase in the short-circuit

Table 1. Obtained parameters from the analysis capacitance spectra data considering Eqs. 3 and 5.

Incident light				
Average wavelength (nm)	Intensity (μW/cm^2)	n^*/n_0	$ln(\omega_0)$	L_D (nm)
409	250	3.6×10^3	6.88	6.2
	480	6.1×10^3	7.41	
475	200	2.6×10^3	6.56	9.3
	415	5.4×10^3	7.28	
523	150	2.2×10^3	6.39	2.0
	275	3.2×10^3	6.78	
589	210	4.5×10^2	4.81	19.6
	86	7.8×10^2	5.36	

current at different illumination levels. Only the free charge-carrier densities of holes where considered in these calculations because, even though the photogenerated charge density is equal for both electrons and holes, due to the higher mobility of holes in devices built in a similar structure [14], only free holes will contribute to the change of the occupancy of the states that can be probed by the capacitance measurement.

One interesting result is obtained for the Debye length associated to the bulk quasi-Fermi level when the device is illuminated by light at 523 nm. The Debye length obtained is considerably smaller (2 nm) than the obtained under illumination at other wavelength ranges. This smaller value of the Debye length is responsible to the higher dispersion in the capacitance spectra, in spite of the lower n^*/n_0 ratio. Such a shorter Debye length can be associated to the fact that the polymer optical bandgap edge coincides with the wavelength range of the excitation source. In such situation, the photocurrent response of OLEDs follows an *antibatic* behavior, in contrast to the *symbatic* [4, 6] behavior expected for excitation in wavelengths far from the bandgap edge.

Conclusions

The application of an abrupt cut-off frequency model for the interpretation of the frequency-dependent capacitance of devices comprising a rectifying junction has been successfully adapted to analyze the results obtained from polymeric electronic devices under illumination. The effect of light-excitation shifts the quasi-Fermi levels towards the corresponding band edges, allowing states which could not be probed by admittance/capacitance measurement to follow the a.c. modulation and change their occupancy condition. Using this adapted formalism, it was possible to determine the ratio between the photo-generated free charge-carrier density and the intrinsic charge-carrier density (or the displacement in the quasi-Fermi level), the bulk Fermi level position and the Debye length associated to the states which cross the bulk quasi-Fermi level. Further experiments considering the variation of parameters, like, for instance, the device thickness or experimental conditions like the temperature would be interesting to know the real extension of the adaptation to the model made in the present work.

Acknowledgments

The authors acknowledge the resources obtained from the financial support of the Brazilian agencies FAPESP (grant # 09/16052-4) and CNPq (grant # 476718/2010-4). C.J.P. thanks CAPES for the granted scholarship. L.F.S. thanks the research fellowships granted by CNPq (grant # 305027/2009-3) and CAPES (grant # BEX 0559/11-3).

References

[1] Barth, S., Bässler, H. (1997). *Phys. Rev. Lett.*, *79*, 4445.
[2] Nespurek, S., Cimrova, V., Pfleger, J., Kiminek, I. (1996). *Pol. Adv. Tech.*, *7*, 459.
[3] Chandross, M., Mazumdar, S., Jeglinski, S., Wei, X., Vardeny, Z.V., Kwock, E.W., Miller, T.M. (1994). *Phys. Rev. B*, *50*, 14702.
[4] Harrison, M. G., Gruner, J., Spencer, G.C.W. (1997). *Phys. Rev. B*, *55*, 7831.
[5] Lee, S. B., Yoshino, K., Park, J. Y., Park, Y. W. (2000). *Phys. Rev. B*, *61*, 2151.
[6] Cazati, T., Santos, L. F., Reis, F. T., Faria, R. M. (2012). *Appl. Phys. A*, *108*, 545.
[7] Chawdhury, N., Köhler, A., Harrison, M. G., Hwang, D. H., Holmes, A. B., Friend, R. H. (1999). *Synth. Met.*, *102*, 871.

[8] Garcia-Belmonte, G., Boix, P. P., Bisquert, J., Sessolo, M., Bolink, H. J. (2010). *Sol. Energ. Mat. & Sol. Cells*, *94*, 366.
[9] Shah, M., Karimov, Kh. S., Sayyad, M. H. (2010). *Semicond. Sci. Technol*., *25*, 075014.
[10] Cohen, J. D., Lang D. V. (1982). *Phys. Rev. B*, *25*, 5321.
[11] Mencaraglia, D., Ould Saad, S., Djebbour, Z. (2003). *Thin Solid Films*, *431-432*, 135.
[12] Reis, F. T., Mencaraglia, D., Ould Saad, S., Séguy, I., Oukachmih, M., Jolinat, P., Destruel, P. (2003). *Synth. Met*., *138*, 33.
[13] Reis, F. T., Santos, L. F., Bianchi, R. F., Cunha, H. N., Mencaraglia, D., Faria, R. M. (2009). *Appl. Phys. A*, *96*, 909.
[14] Santos, L. F., Faria, R. M., de Andrade, A. R., Faria, G. C., Amorin, C. A., Mergulhão, S. (2007). *Thin Solid Films*, *515*, 8034.